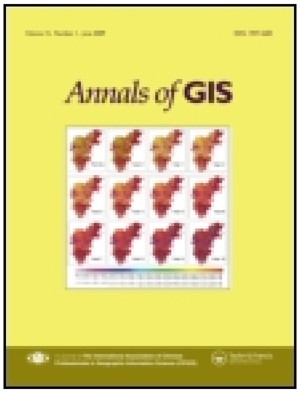

Annals of GIS
Publication details, including instructions for authors and subscription information:
http://www.tandfonline.com/loi/tagi20

Depicting classification uncertainty using perception-based color models

James E. Burt [a] , A-Xing Zhu [a b] & Mark Harrower [a]
[a] Department of Geography, University of Wisconsin-Madison, Madison, WI, USA
[b] State Key Laboratory of Resources and Environmental Information Systems, Institute of Geographical Sciences and Natural Resources Research, Chinese Academy of Sciences, Beijing, PR China

Available online: 26 Sep 2011

Annals of GIS
Vol. 17, No. 3, September 2011, 147–153

Depicting classification uncertainty using perception-based color models

James E. Burt[a], A-Xing Zhu[a,b]* and Mark Harrower[a]

[a]*Department of Geography, University of Wisconsin-Madison, Madison, WI, USA;* [b]*State Key Laboratory of Resources and Environmental Information Systems, Institute of Geographical Sciences and Natural Resources Research, Chinese Academy of Sciences, Beijing, PR China*

(*Received 20 June 2011; final version received 21 June 2011*)

Fuzzy classification typically assigns a location or an area to a category with some estimated degree of uncertainty. There are strong incentives for depicting uncertainty along with category, and numerous authors have recommended that this be done using progressive desaturation of the entity's color with increasing uncertainty. This article shows that such recommendations cannot be naively applied using color models widely used in computer graphics because colors equally 'saturated' do not appear equally certain. We demonstrate that models based on color perception are preferred, particularly if one wishes to compare uncertainties across classes. We discuss geometrical complications arising with perceptual models that are not present with models closely tied to hardware. An algorithm for selecting colors is presented and illustrated using the model.

Keywords: uncertainty; classification; visualization; SoLIM; digital soil mapping (DSM)

1. Introduction

1.1 Background

Fuzzy classification is becoming routine in geographic analysis (such as remote sensing classification and digital soil mapping (DSM)) (Burrough *et al.* 1992, Zhu *et al.* 2001, Zhu 2006). Unlike traditional classification, which implicitly assumes entities are members of a single class, fuzzy classifiers admit membership in multiple classes. Membership values in different classes are often represented in a membership vector, $\boldsymbol{M}_{ij}$ of n-elements, with each element ${m_{ij}}^k$ representing the belonging (or the similarity) of location (i,j) to class k (such as in the SOLIM method) (Zhu *et al.* 2001). Uncertainty is introduced when the location is assigned to a single class, namely to the class in which the location (pixel) has the highest membership, referred as hardening, and this uncertainty can be measured by analyzing the membership vector which was hardened (Zhu 1997).

Typically, along with the category value, an uncertainty value is attached to each entity. As discussed in Zhu (1997), the uncertainty value might be a measure of the distance between the classified entity and a prototype defined for the most similar category (exaggeration uncertainty), or it might index the degree to which the entity has membership in multiple categories (ignorance uncertainty). Consider, for example, a vector (0.25, 0.35, 0.25, 0.15) indicating a pixel's similarity (M) to four classes. The hardening process, as shown in Figure 1, assigns the pixel to class 2, but obviously it exaggerates the membership in that class while deflating membership in the other three classes.

Exaggeration uncertainty indexes this using the departure from full membership in class 2:

$$E = 1 - \max(m_i) = 1 - 0.35 = 0.65 \qquad (1)$$

That is, in claiming sole membership in class 2, we exaggerate by 65%. Alternatively, the ignorance uncertainty is

$$I = -\frac{1}{\log(n)} \sum_{i=1}^{n} m_i * \log(m_i) = 0.97 \qquad (2)$$

indicating that this pixel has relatively uniform membership in multiple categories. That is, I informs a user that the pixel might reasonably be assigned to other classes.

Regardless of how uncertainty is measured, methods are needed for mapping categories along with the associated uncertainties. This article considers methods for accomplishing that in ways that are optimal from a perceptual standpoint. We should emphasize that although the discussion is motivated by fuzzy classification, the following applies to chloropleth mapping in general, whenever a

*Corresponding author. Email: axing@lreis.ac.cn

ISSN 1947-5683 print/ISSN 1947-5691 online

http://dx.doi.org/10.1080/19475683.2011.602024
http://www.tandfonline.com

$$M = (0.25, 0.35, 0.25, 0.15) \xrightarrow{\text{Hardening}} (0, 1, 0, 0)$$

Figure 1. Hardening of a membership vector into a single class.

normalized uncertainty value can be assigned to attribute data. That is, the only requirement is that uncertainty be expressed on the same finite scale for all classes.

1.2 The issue

Our goal is effective presentation and visualization of category and uncertainty on the same map. This is hardly a new problem, and various authors have suggested that decreasing color saturation can be used to indicate progressively larger amounts of uncertainty (see McEachren, 1992, Goodchild *et al.* 1994, Leitner and Buttenfield 2001). That is, an entity having no uncertainty appears as a fully saturated color, whereas total uncertainty is rendered in a monochrome color. This can be readily accomplished using tools available in common mapping, Geographical Information System (GIS), and illustration software, almost all of which provide the ability to define color in Hue-Saturation-Value (HSV), Hue-Lightness-Saturation (HLS), or a similar system that explicitly contains 'saturation' as a variable (Foley *et al.* 1996). However, such color systems have been developed for ease of use, and are not tied to any absolute standard of color or psychophysical response. For example, fully saturated red is mapped to whatever the most 'pure' red the current display device can produce, without reference to any color standard nor is there any consideration of how that color will be perceived. Thus, there is no guarantee that a 50% saturated red will appear equally uncertain as a 50% saturated yellow. In fact, because the HSV and HLS systems conflate luminance (lightness) and saturation, we can be sure that they will not. This is seen in Figure 2, which shows the top of the HSV cone. If the models were perceptually accurate, luminance would decrease outward in concentric rings. The appearance of brighter and darker 'rays' of luminance in some directions indicates that this model fails on perceptual grounds.

The basic difficulty is that in some directions (i.e., for some hues) a unit change in saturation gives a larger change in luminance than others. The result is that apparent certainty – or equivalently, the perceptual distance from white – varies non-uniformly with hue.

2 Methodology

Fortunately, a number of perception-based color models exist, including Munsell, the Commission Internationale de l'Eclairage (CIE) systems $L^*a^*b^*$ and $L^*u^*v^*$, and Ljg system of the Optical Society of America (Nickerson 1981, Hunt 1995). These systems are similar in that they are tied to a prescribed color standard, and thus the colors associated with a particular point in the color model are not dependent on the properties of the display device. These

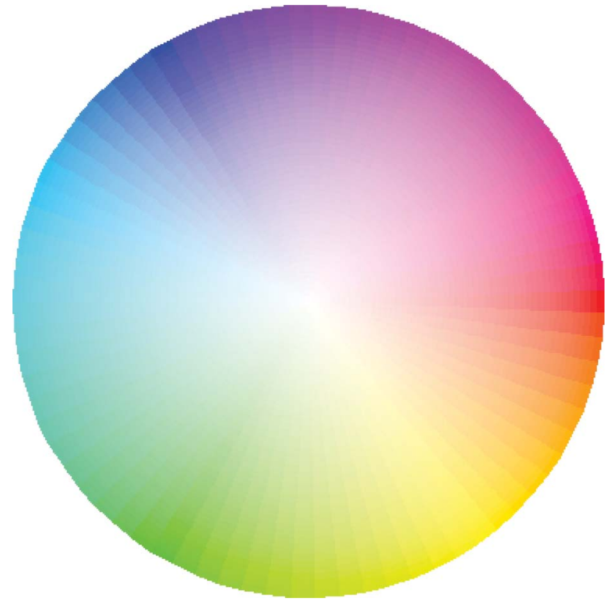

Figure 2. Full-value colors of the HSV model. (Color version available online.)

are also similar in that all are three-dimensional models in which a unit change in any direction is supposed to give a uniform perceptual change. Finally, all contain a luminance axis perpendicular to two other orthogonal axes that in combination yield the hue of a color.

The perception-based models differ in several important ways. First, their coordinate axes are not identical in terms of numerical value. For example, the luminance axis of the Munsell system ranges from 0 (black) to 10 (white), whereas the corresponding L^* axes of the two CIE systems range from 0 to 100, and L of the Ljg system admits negative as well as positive values. The axes controlling the chromacity (or color hue) are different in all systems. Although conversion between systems is possible, such transformations are nonlinear and do not involve simple scaling of corresponding axes. (The exception is L^*, which is the same in both $L^*a^*b^*$ and $L^*u^*v^*$.) A more important difference is that the systems rest on different experiments involving color perception of test subjects. It would therefore be difficult to claim one system as clearly superior to the others, and this article considers all the perceptual systems as potentially useful in rendering uncertainty.

We can exploit the fact that in all models monochrome colors are found along the luminance axis, and increasing saturation is found along radial lines in any plane of constant luminance. Thus, two points equidistant from the luminance axis will in principle have equal perceived uncertainty. In the method proposed here, colors assigned to each soil category will be located on a ray originating at the luminance axis. Total uncertainty will be indicated by points at the origin, with colors for progressively more certain pixels chosen progressively farther along the ray. We propose that this approach provides a better basis for rendering uncertainty than methods based on hardware-related models such as HSV or HLS.

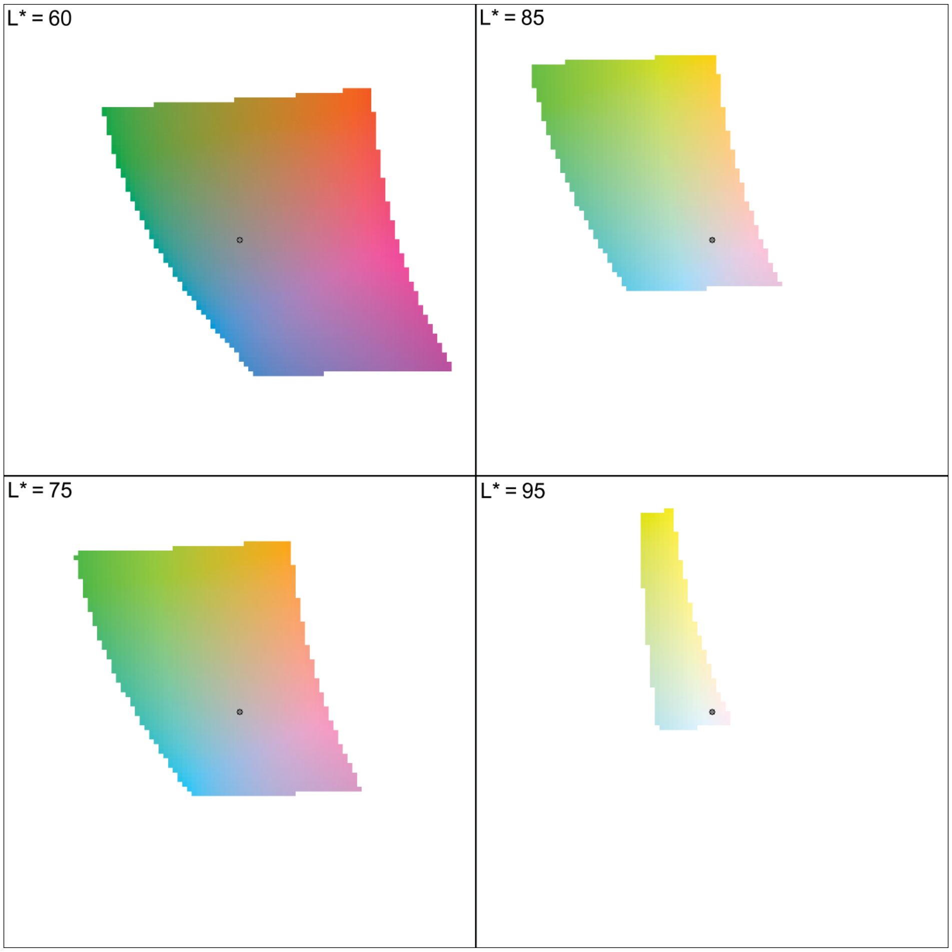

Figure 3. Cross sections of the $L^*a^*b^*$ space for various luminance values. Dots in each cross section are placed at the origin $a^* = b^* = 0$, corresponding to total uncertainty. (Color version available online.)

Application of this approach is complicated by the fact that the universe of possible colors in these models is bounded by an irregular three-dimensional solid. For example, Figure 3 shows slices of the $L^*a^*b^*$ system for a few values of L^*.

The cross sections are centered with respect to one another, meaning that the gray points ($a^* = b^* = 0$) are in the center of each square. Figure 4 shows similar cross sections for the Munsell system. Note that in both of these systems, one can move radially from the origin with little or no apparent change in luminance. Thus, in contrast to what is seen in Figure 2, these systems are much closer to offering saturation values proportional to perceived uncertainty.

Note that in Figures 3 and 4, the maximum distance possible, that is, the maximum saturation possible, depends heavily on luminance and hue. Similar conclusions hold for the $L^*u^*v^*$ and Ljg systems (not shown). We propose that for any luminance value, pixels with complete certainty (unity) should be located as far as possible from the monochrome point. This will obviously maximize the range in perceived uncertainty, and thereby maximize the visual resolution in uncertainty. Another requirement is that any two pixels having the same uncertainty should be as far as possible from each other in the color space. Taken together, these requirements mean that fully saturated colors will be equally spaced along a circle centered on the origin. Reflecting this, our basic algorithm is as follows:

Given the number of classes n ($n > 1$):

(1) Define the angle between hues $\beta = 360°/n$
(2) Select a luminance value L^* or L.
(3) Search for optimum equally spaced directions α_1, $\alpha_2, \ldots, \alpha_n$ where $\alpha_i = \alpha_{i-1} + \beta$:
  (a) Initialize $S_{\max} = 0$
  (b) For $\mu = 1°, 2°, \ldots \beta$ try $\alpha_1 = \mu$, $\alpha_2 = \mu + \beta$, ...
  (c) Find $S_{\min}$, the minimum saturation possible for $\alpha_1, \alpha_2, \ldots, \alpha_n$. If $S_{\min} > S_{\max}$, save μ as μ_{opt} and assign $S_{\min} = S_{\max}$.
  (d) Let $\alpha_i = i\,(\mu_{opt})$, $i = 1, 2, \ldots n$

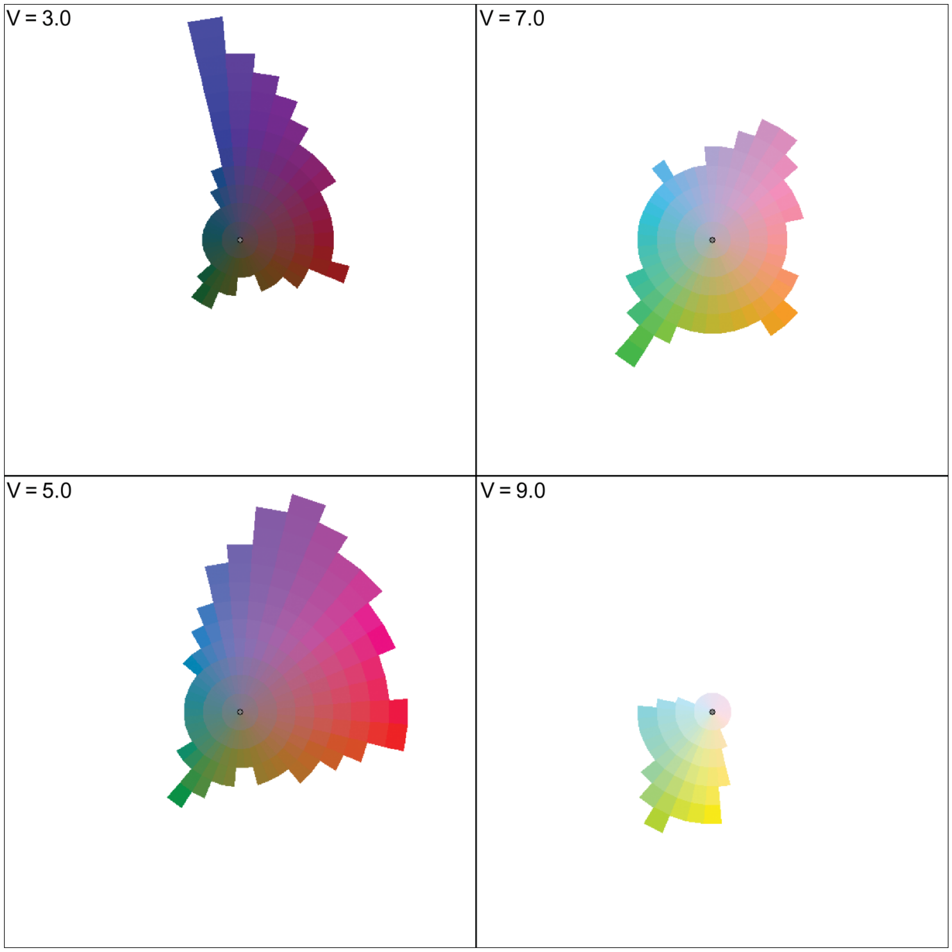

Figure 4. Cross sections for the Munsell system. (Color version available online.)

This process gives n colors on the circumference of a circle whose radius is just small enough to ensure that all n colors are realizable. As an example, consider Figure 5, which shows the colors that result for a map with $n = 3$ (three classes).

The dots indicate colors that would be used for pixels with no uncertainty. All are equidistant from gray, and thus have equal saturation. However, only one of them – the upper, left point – has the maximum saturation possible for its hue. The other two points are somewhat undersaturated relative to what is possible. For example, the dot in the reddish-pink area is considerably inside the color slice. A ray connecting the origin and that dot intersects many colors outside the circle. Those colors are all more saturated than any point on the circle. Using those colors would give a mistaken impression of greater certainty, and thus they should be avoided. The fact that the circle of total certainty crosses outside the envelope of possible colors is of no consequence. A map would contain only colors along rays from the dots to the origin.

3 Implementation and results

3.1 *Basic method*

The algorithm has been implemented as a C++ program for MS Windows and is available from http:\\solim.geography.wisc.edu\software\ The program computes colors for a variable number of classes in the $L^*u^*v^*$, $L^*a^*b^*$, and Ljg models, as well as for HSV.

The search algorithm was implemented as indicated, with no attempt at optimization. Therefore the slow search method, along with the complexities of converting from perceptual coordinates to RGB, means the approach cannot be used as coded in real-time applications. In particular, on a personal computer the program requires 2–3 seconds to identify and display a full suite of colors for all four models. However, in most instances the classification process generating the map data will be very slow by comparison, thus efficiency in choosing colors is not a factor.

Figure 6 is an example of the output showing just the panels for the Ljg and HSV models. Moving horizontally across the color bars at constant saturation, there would

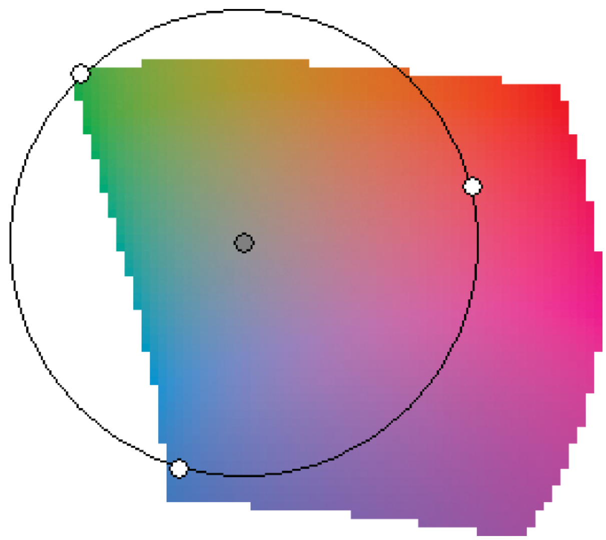

Figure 5. Cross section of Ljg for $L = 50$ showing optimum color choices for three classes. Pixels for a class would be chosen from colors along rays connecting a point and the origin (center dot). (Color version available online.)

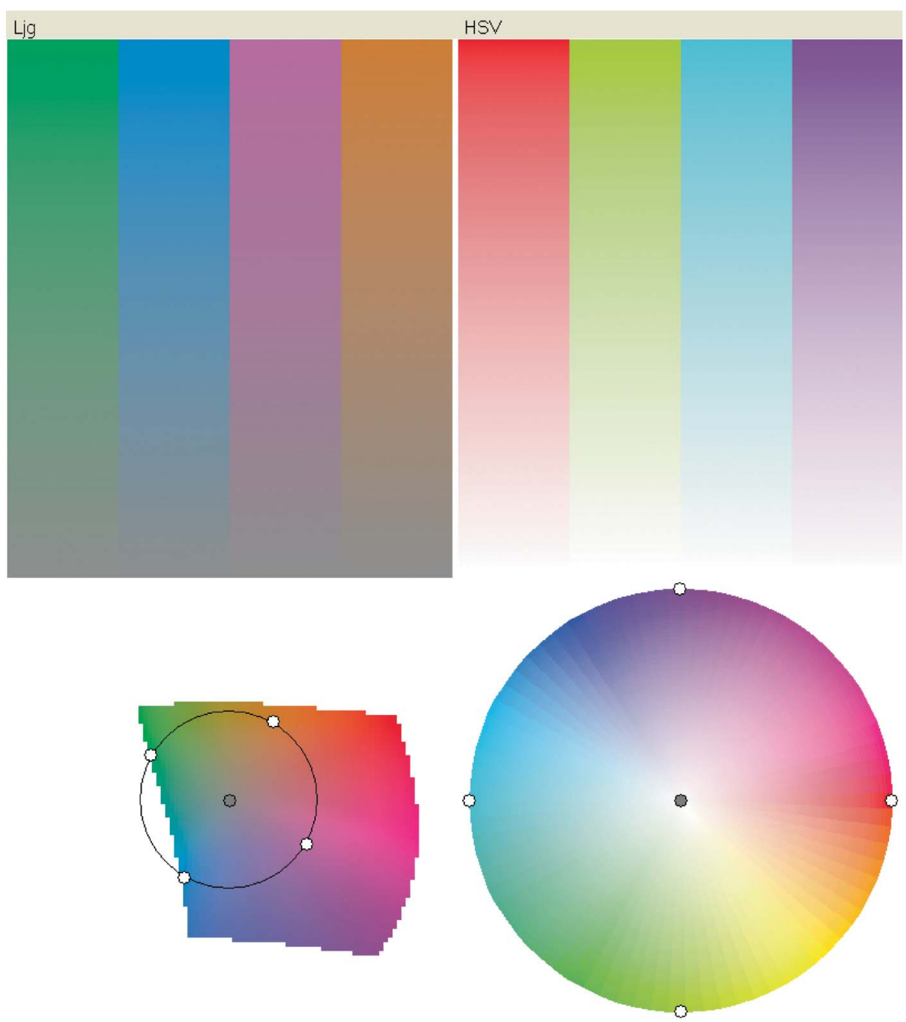

Figure 6. Color gamuts from the Ljg (left) and HSV (right) models for a four-category map. (Color version available online.)

ideally be no change in perceived uncertainty. For example, moving across the top of the HSV bars, the green bar appears less certain than either the red bar or the purple bar. In addition, moving downward, the red bar desaturates rapidly at the top and more slowly with depth. Ideally, there would be a linear perceptual change with increasing distance from the top. At least for the authors, the Ljg bars come significantly closer to that ideal than the HSV bars shown in Figure 6.

We have done no formal testing, but our examination of results for $n = 2, 3, \ldots, 12$ confirms that three perceptual models always out-perform HSV in this regard.

Our primary result, therefore, is to provide evidence that the theoretical advantages of perception-based models very likely translate into actual advantages. We recognize that the question will only be answered definitively by a carefully controlled study using human subjects. We believe that our results provide support for such future studies. In addition, our subjective analysis suggests that Ljg model is preferred, but we are not prepared to claim its superiority over the two CIE models. Again, that needs to be answered by more study. In addition, such studies need to investigate whether continuous variation in saturation is best. It might be that only a few saturation classes would be preferable.

As another example, consider Figure 7, which results from applying the method to a 10-class soils map displayed using 3dMapper (Terrain Analytics 2001). Note that the combination of class and uncertainty provides important information that would be hard to obtain from either map alone. For example, in many locations there is a gradual transition through zones of uncertainty, indicating intermediate soils that do not fall neatly into any category. But in other places there is a sharp break from relatively certain to uncertain following abrupt changes in bedrock control. Notice also that this map raises the question of whether synthetic hill-shading is advantageous. It obviously provides important clues about landform, but shadows move pixel colors down the luminance axis, which has the potential to be interpreted as increasing uncertainty. Our strong inclination is therefore to provide shading only in interactive environments, where the effective sun position can be easily varied, and even in those instances we recommend providing shading as an option that can easily be toggled on and off, as with 3dMapper.

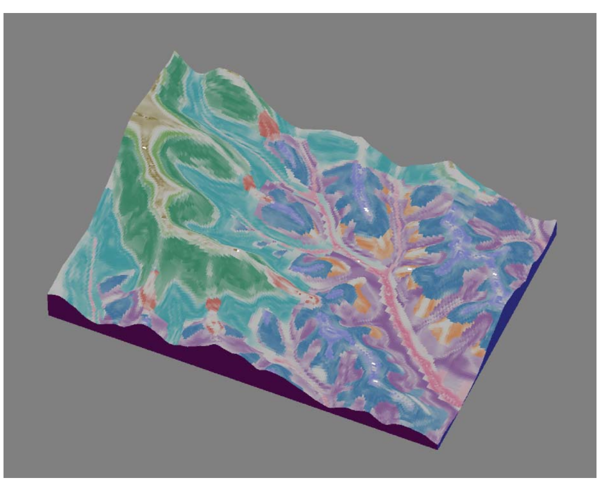

Figure 7. A combined category/uncertainty map. Different hues represent different soil types and different levels of saturation represents different levels of certainty in the class. (Color version available online.)

3.2 Enhancements

There are two obvious enhancements, both of which are useful for increasing the dynamic range of colors available. As we have indicated, each class has a range of colors lying along a line running from achromatic to the maximum possible saturation, which is the same for all classes. To increase the range of colors, we need to lengthen that line.

One obvious way to increase the range is to search for a luminance value that gives as large a radius as possible. In other words, for a given n, we need to find an L^* or L that maximizes the radius $S_{\max}$. That is easily accomplished by replacing Step 2 in the algorithm with a line search along the luminance axis. For every trial point along the axis, we examine the cross section to find the largest radius possible for that luminance. The maximum over all luminance values reveals the optimum luminance.

Another way to increase the range is to use white as the origin of every color bar. That is, instead of holding luminance fixed along the color bar, we allow luminance increase, with white rather than some gray level as the color associated with maximum uncertainty. Geometrically, we

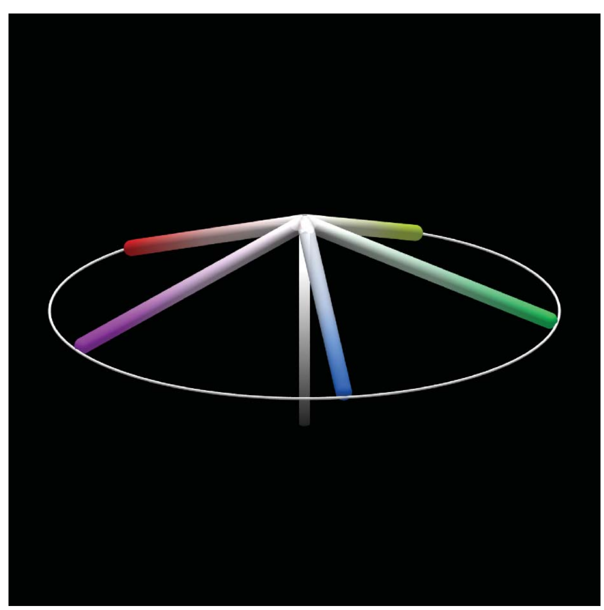

Figure 8. Color bars forced to terminate on white. (Color version available online.)

allow the bars to slant upward from the optimum luminance to white, which obviously lengthens each bar (see Figure 8).

Note that because they cross luminance values, it is possible for a bar to exit the volume of realizable colors. Our code checks for that, and displays a warning message when it occurs. As a practical matter, this might not be a significant issue – at least we did not encounter the problem in any of our testing. This follows from the fact that the intersections of the color volumes and a plane running through the luminance axis are not too far from convex. (Figure 3 gives some hint of that.) Note also that the color bars could be extended by terminating them at a lower luminance value, that is, at a darker gray or even black. Our subjective evaluation is that this tends to overly obscure differences in hue to the point that the base class becomes difficult to ascertain.

4 Conclusions

We argue that perceptual color models such as $L^*u^*v^*$ and Ljg are better choices for displaying class uncertainty than other more commonly used models such as HSV or HLS. Although they are not suitable for real-time display, perceptual models have a strong advantage in maps whose categories and uncertainties are fixed. That is, they are indisputably superior on theoretical grounds because they are designed to give the appropriate psychophysical response. The informal evaluations reported here are entirely consistent with that advantage, but further work using human subject testing is needed for confirmation. Human testing is also needed to examine an assumption that we have not discussed, namely whether saturation in a perceptual model scales linearly to perceived uncertainty. For example, we wonder if 40% saturation is perceived to be twice as uncertain as 20% saturation. The models are designed so that the perceived colors have the proper relationship, but we do not know how color is mapped to the perception of uncertainty.

It is important to emphasize that our study is narrowly focused on pixel-level display of uncertainty. Accordingly, it considers only saturation as a visual variable to be manipulated in conveying uncertainty. Other variables (e.g., texture, crispness, resolution) cited as useful for uncertainty cannot be applied at the pixel level (see Slocum 1999, pp. 242–249). We do not mean to imply that saturation is the best variable for rendering uncertainty in other situations, such as when mapping point or boundary placement. Rather, our goal has been to provide guidance regarding how saturation can best be used for pixel uncertainty, given that it appears to be the only logical candidate.

We close by noting that in addition to situations like those described here, where uncertainty is generated as part of some discrete classification process, our method has utility when a continuous attribute value is imprecise. For example, in Nemani *et al.* (2003) purity of color was used to indicate the relative contribution of three variables to net ecosystem productivity. We believe that a continuum anchored in a perceptual model is appropriate for such maps.

Acknowledgments

The financial and logistical supports from the USDA Natural Resources Conservation Service and the Chinese Academy of Sciences through its 'One-Hundred Talent Program', from the Vilas Associates program and the Hamel Faculty Fellow program of University of Wisconsin-Madison are gratefully acknowledged.

References

Burrough, P.A., Macmillan, R.A., and van Deursen, W., 1992. Fuzzy classification methods for determining land suitability from soil profile observations and topography. *Journal of Soil Science*, 43, 193–210.

Foley, J.D., et al. 1996. *Computer graphics: Principles and practice in C*. 2nd ed. Reading, MA: Addison-Wesley, 1177 p.

Goodchild, M., Buttenfield, B., and Wood, J., 1994. Introduction to visualizing data uncertainty. Chapter 15. *In*: H.M. Hearnshaw and D.J. Unwin, eds. *Visualization in geographical information systems*. Chichester, UK: Association for Geographic Education (Wiley), 141–149.

Hunt, R.W.G., 1995. *The reproduction of color*. 5th ed. Kingston-upon-Thames. England: Fountain.

Leitner, M. and Buttenfield, B., 2001. Guidelines for the display of attribute uncertainty. *Cartography and Geographic Information Science*, 27, 3–14.

McEachren, A.M., 1992. Visualizing uncertain information. *Cartographic Perspectives*, 13, 10–19.

Nemani, R.R., et al. 2003. Climate-driven increases in global terrestrial net primary production from 1982 to 1999. *Science*, 300, 1560–1563.

Nickerson, D., 1981. OSA uniform color scale samples: a unique set. *Color Research and Application*, 6, 7–33.

Slocum, T.A., 1999. *Thematic cartography and visualization*. New York: Prentice-Hall, 293 p.

Terrain Analytics, 2001. 3dMapper: Software for 3-d landscape visualization and mapping. Available from: www.TerrainAnalytics.com.

Zhu, A.X., 1997. Measuring uncertainty in class assignment for natural resource maps using a similarity model. *Photogrammetric Engineering & Remote Sensing*, 63, 1195–1202.

Zhu, A.X., 2006. Fuzzy logic models in soil science. *In*: S. Grunwald and M.E. Collins, eds. *Environmental soil-landscape modeling: geographic information technologies and pedometrics*. New York: CRC/Taylor & Francis, pp. 215–239.

Zhu, A.X., et al. 2001. Soil mapping using GIS, expert knowledge, and fuzzy logic. *Soil Science Society of America Journal*, 65, 1463–1472.